Available online at www.sciencedirect.com

ScienceDirect

Procedia Engineering 158 (2016) 362 – 367

Procedia Engineering

www.elsevier.com/locate/procedia

VI ITALIAN CONFERENCE OF RESEARCHERS IN GEOTECHNICAL ENGINEERING – Geotechnical Engineering in Multidisciplinary Research: from Microscale to Regional Scale, CNRIG2016

Seismic performance of the San Pietro dam

Domenico Aliberti[a,]*, Ernesto Cascone[a], Giovanni Biondi[a]

[a]*University of Messina, Contrada di Dio, S.Agata, 98166 Messina, Italy*

Abstract

The paper focuses on the seismic performance of the San Pietro dam (located in Southern Italy) evaluated, with different levels of accuracy, through pseudo-static, simplified-displacement and dynamic 2D finite difference analyses. For critical mechanisms, detected through pseudo-static analyses, simplified displacement analyses were performed assessing the horizontal and vertical components of the expected permanent displacements. Dynamic analyses were carried out accounting for non-linear soil behavior under cyclic loading. The adopted input motions consist of several sets of accelerograms selected, from a worldwide database, assuming as a reference the seismicity of the area where the dam is located. The results of the analyses show a satisfactory behavior of the dam for the selected input motions.

Peer-review under the responsibility of the organizing and scientific committees of CNRIG2016

Keywords: Earth dam; seismic analysis; permanent displacements

1. Introduction

The San Pietro dam is a zoned earth dam located in Campania (Southern Italy) along the river Osento, in a high seismicity area. The embankment of the dam (49 m high) was built between 1958 and 1964 has a volume of about 2.2 Mm^3 and retains 17.7 Mm^3 of water with a freeboard of 1.5 m. The main cross section of the dam is shown in Figure 1. The geotechnical characterization of the foundation soils and of the dam is based on the results of recent investigations [1]. The core is made of low plasticity clayey silts, the shells are made of granular soils and the foundation soil consists of a layer of alluvial gravels (improved by concrete injections under the dam), overlying a

* Corresponding author. Tel.: +39-090-3977585.
E-mail address: daliberti@unime.it

Peer-review under the responsibility of the organizing and scientific committees of CNRIG2016
doi:10.1016/j.proeng.2016.08.456

deep stiff overconsolidated flysch deposit. The seismic performance of the dam was checked through pseudo-static analyses, simplified displacements analyses and dynamic 2D numerical analyses carried out, with reference to the main cross section of the dam, using the code FLAC 2D v.7.0 [2]. Some of the obtained results are described herein.

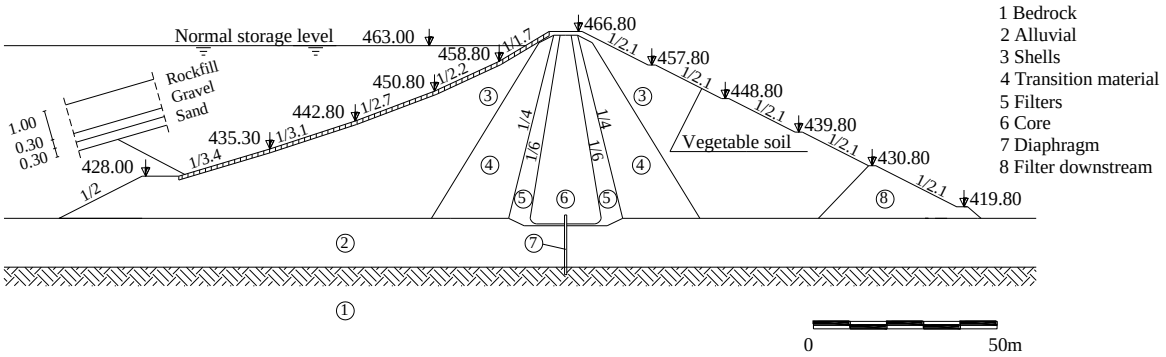

Fig. 1. Cross section of the dam (adapted from Calabresi et al. [1]).

2. Selection of input motions

According to the prescription of the Italian technical code [3,4], the seismic analyses were carried out considering the *Collapse Limit State* (*CLS*), the *Life Safety Limit State* (*LLS*) and the *Damage Limit State* (*DLS*). Only the results relative to the *CLS* and *LLS* will be presented herein. For these two limit states the expected peak values of the horizontal acceleration at the dam site are 0.414 *g* and 0.304 *g*, respectively.

The adopted input motions were selected from an Italian [5] and a worldwide [6] database. Moment magnitude M_w and Joyner & Boore [7] site-source distance d_{JB} were initially considered as selection parameters assuming $6 \le M_w \le 7$ and $1 \text{ km} \le d_{JB} \le 15$ km according to the seismic hazard disaggregation data provided by the Italian Seismic Hazard Map [8]. The selection was further refined, according to [9] and [10], checking the similarity between the elastic response spectrum of each of the selected accelerogram and a target response spectrum provided by the Italian code for the site at hand and for a given limit state. The similarity was checked in terms of compatibility of the peak horizontal acceleration (i.e. the spectral ordinate for $T = 0$ s), quantified through an acceleration scale factor F_S, and in terms of deviation between the response spectrum of the selected accelerogram and the target spectrum, measured by the Pearson correlation index R^2 and by the average root-mean square deviation D_{rms}, the latter was evaluated in the range $T = 0.1 \div 0.5$ s since the natural period of the dam is $T_1 = 0.32$ s.

The results of the accelerogram selection are shown in Table 1 and in Figure 2. It can be observed that the limitations $F_s \le 2.0$, $R^2 \ge 0.8$, $D_{rms} \le 0.10$ (light grey area in Fig. 2), adopted according to [9] and [10], allow detecting only one accelerogram (#1) for the *CLS* and only three accelerograms (#4, #5, #6) for the *LLS*. To obtain larger sets of accelerograms the limits of the selection parameters were enlarged, assuming $F_s \le 2.5$, $R^2 \ge 0.8$, $D_{rms} \le 0.15$ for the *CLS* and $F_s \le 2$, $R^2 \ge 0.8$, $D_{rms} \le 0.15$ for the *LLS*; thus, the two sets of five accelerograms listed in Table 1 was finally obtained. Some of the selected records (#3, #4 and #5) fit the adopted limitations for both the *CLS* and the *LLS*. The values of the mean period T_m, of the Arias intensity I_a and of the destructiveness potential factor P_d, evaluated for the scaled accelerograms, are also listed in Table 1.

3. Numerical model

All the numerical analyses presented in the paper were carried out using the computer code FLAC 2D v.7.0 [2] discretizing the dam and the foundation soils over a finite difference mesh of 13845 quadrilateral elements. The pore pressure distribution in the foundation soils, before the dam construction, was assumed hydrostatic with the water table at the original ground surface.

Table. 1. Result of the accelerogram selection for the *CLS* (a,b) and the *LLS* (c,d) and main parameters of the scaled accelerograms.

N.	Earthquake	Station – record (date)	M_w (-)	a_{max} *(g)*	F_S (-)	R^2 (-)	D_{rms} (-)	T_m (s)	I_A (m/s)	P_D (10^{-4}g·s^3)
CLS (a_{max} = 0.414 *g*): 6.0 ≤ M_w ≤ 7.0 , 1 km ≤ d_{JB} ≤ 25 km										
#1	Loma Prieta	Gilroy Array # 1 – 000 (18/10/1989)	6.9	0.411	1.008	0.817	0.072	0.290	1.07	5.63
#2	Loma Prieta	Gilroy Array # 1 – 090 (18/10/1989)	6.9	0.473	0.875	0.843	0.148	0.387	1.29	11.09
#3	Parkfield -02 CA	Parkfield – Turkey Flat # 1 – 270 (28/09/2004)	6.0	0.245	1.688	0.908	0.106	0.366	0.49	3.40
#4	Parkfield -02 CA	Parkfield – Turkey Flat # 1 – 360 (28/09/2004)	6.0	0.196	2.111	0.900	0.095	0.449	0.84	10.96
#5	Northridge	Wonderland Ave – 185 (17/01/1994)	6.7	0.172	2.406	0.941	0.087	0.448	1.16	13.28
LLS (a_{max} = 0.304 *g*): 6.0 ≤ M_w ≤ 7.0 , 1 km ≤ d_{JB} ≤ 25 km										
#3	Parkfield -02 CA	Parkfield – Turkey Flat # 1 – 270 (28/09/2004)	6.0	0.245	1.239	0.913	0.106	0.366	0.26	1.83
#4	Parkfield -02 CA	Parkfield – Turkey Flat # 1 – 360 (28/09/2004)	6.0	0.196	1.550	0.888	0.099	0.449	0.45	5.91
#5	Northridge	Wonderland Ave – 185 (17/01/1994)	6.7	0.172	1.766	0.935	0.087	0.448	0.63	7.16
#6	Iwate, Japan	IWT010 – NS (13/06/2008)	6.9	0.226	1.348	0.929	0.065	0.517	2.38	16.01
#7	Tottori Japan	SMNH10 – EW (06/10/2000)	6.6	0.231	1.318	0.809	0.140	0.500	0.84	14.82

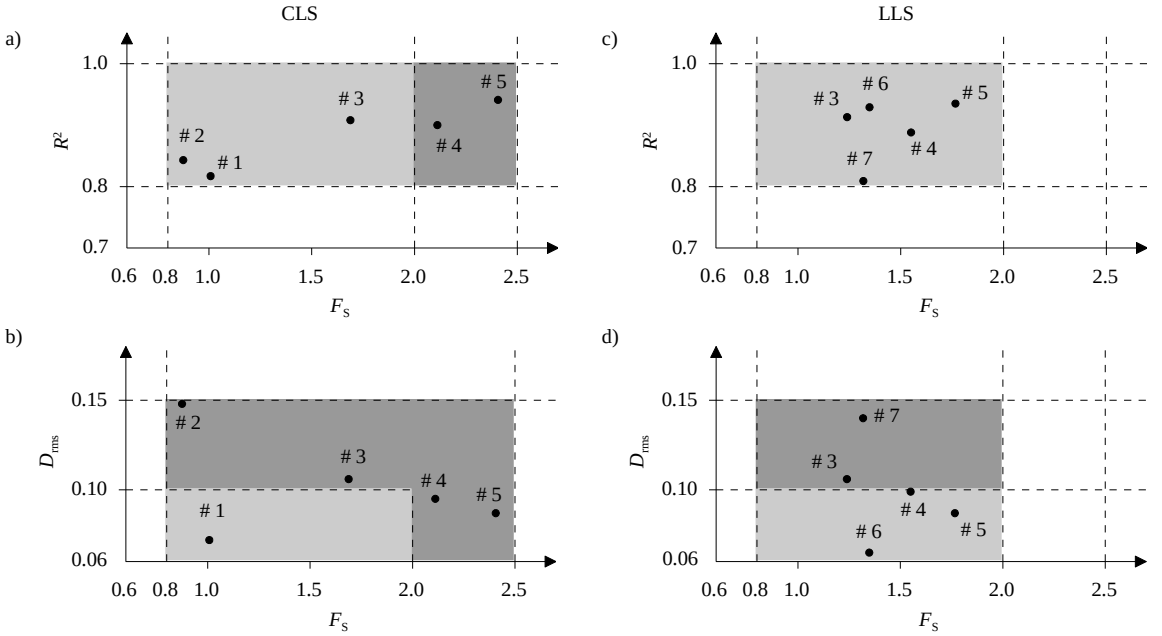

Fig. 2. Result of the accelerogram selection for the *CLS* (a,b) and the *LLS* (c,d).

To reproduce the total and the effective state of stress at the end of the dam construction, a preliminary static analysis was carried out simulating the staged construction as a drained process, via the progressive activation of 12 rows of mesh elements (about 4.0 m thick each), the impoundment of the reservoir and, finally, the ensuing steady state seepage flow. Vertical boundaries were restrained in the horizontal direction, while displacements of the bottom of the mesh were restrained both horizontally and vertically. In the static analysis both the dam and the foundation soils were modeled as an elasto-perfectly plastic material obeying the Mohr-Coulomb failure criterion. The stiffness in the soils of the core and of the shells was assumed constant with depth and the values of the shear modulus were selected in order to reproduce the vertical displacements measured during the construction of the dam by seven extensometers installed at the centre line and in the downstream and upstream slope of the dam.

The uncoupled dynamic analyses were carried out in the time domain accounting for the non-linear behaviour of soils. The values of the small strain shear modulus G_0 were evaluated starting from the results of the cross-hole tests

CH3, *CH4* and *CH5* shown in Figure 3. For the dam body and for the shells, the *CH* data were fitted by a power relationship describing G_0 as a function of the mean effective pressure obtained in the static analyses. As shown in Figure 3a, G_0 exhibits a modest variability with depth in the alluvial deposit; thus, constant values equal to G_0 = 1100 MPa, in the soils directly underlying the dam, and G_0 = 560 MPa, in the soils aside the foundation of the dam, were assumed in the dynamic analyses. The larger value assumed for the soils under the dam can be ascribed to the state of stress induced by the presence of the embankment and to the stiffening effect due to the concrete injections. Finally, also for the bedrock a constant value of G_0 = 1100 MPa was considered (Fig. 3).

To avoid numerical distortion of the propagating wave in the dynamic analysis, the maximum height of elements was assumed smaller than 1/6 of the wavelength λ_{min} associated with the highest frequency f_{max} of the input motion. The mesh extended laterally to about three times the width of the base of the embankment (where the influence of the earth dam is negligible) and at the bottom to a depth of 25 m. At the bottom of the mesh vertical and horizontal viscous boundary were introduced, while boundaries simulating the free-field response were applied at lateral sides.

In the analyses both the soil of the dam body and the foundation soils were schematized as material obeying the Mohr-Coulomb failure criterion. The non-linear and dissipative behaviour was represented using the hysteretic model *Sigmoidal 3* available in the code library. The model parameters were selected in order to fit some of the curves describing the variation of the normalized shear modulus G/G_0 with the shear strain γ, obtained by resonant column tests for the core [1], and deduced from the literature for the shells and for the foundation soils. Finally, for all the materials a viscous Rayleigh damping was introduced assuming f_{min} equal to the fundamental frequency of the dam f_1 = 3.1 Hz (obtained as the first peak of the elastic transfer function between crest and base) and ξ_{min} = 1.7%.

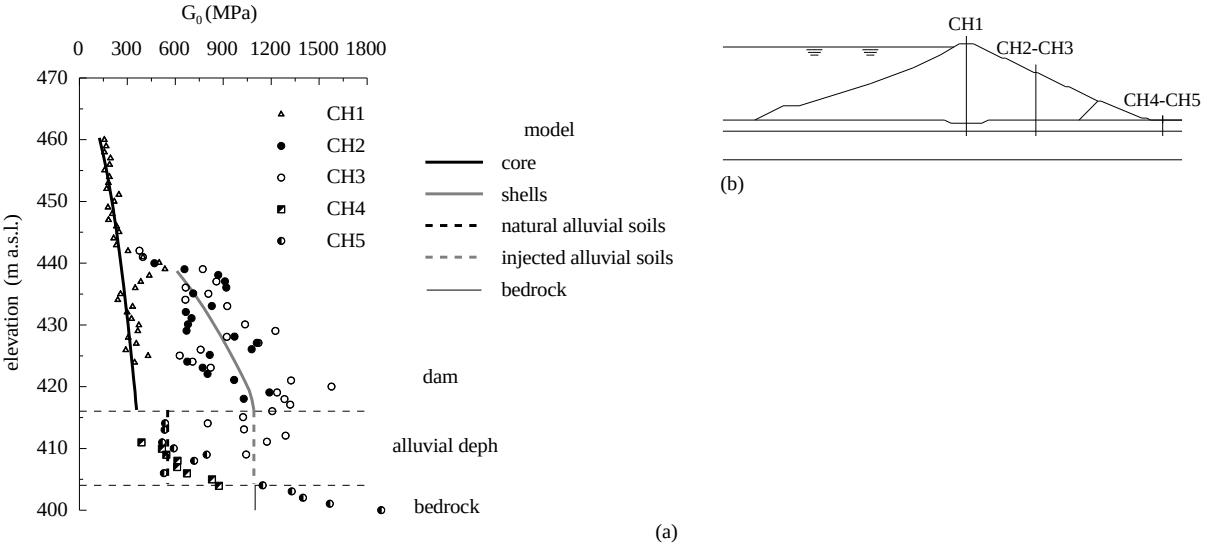

Fig. 3. Results of Cross-Hole test and profiles of G_0 adopted in the seismic analyses.

4. Analysis results

The seismic response of the dam was studied by pseudo-static, simplified-displacement and dynamic 2D finite difference (FD) analyses. Herein, the results of the pseudo-static analyses are omitted.

4.1. Simplified displacement methods

Values of the expected permanent displacement were evaluated through several empirical relationships using the selected input motions. Specifically, the relationships provided by Crespellani et al. [11], Rampello & Callisto [12], Saygili & Rathje [13], Madiai [14] and by Biondi et al. [15], with reference to a rigid block analysis, were considered together with the relationships proposed by Ausilio et al. [16] and by Rathje & Antonakos [17], starting

from a decoupled rigid block analysis, and by Bray & Travasarou [18] through a coupled stick-slip analysis. These relationships correlate the expected permanent displacement u_o of a block sliding on a horizontal plane to the horizontal component of the yield acceleration $a_c = k_{h,c}\, g$ and to some suitable seismic parameters describing the energy and the frequency content of the input motion. A shape factor S is then introduced to account for the actual plastic mechanism, leading to the horizontal (u_x) and vertical (u_y) components of the permanent displacement $u = S \cdot u_o$ of the soil mass.

The horizontal component $k_{h,c}$ of the yield acceleration coefficient, corresponding to the condition of incipient failure, was evaluated through pseudo-static analyses by increasing the horizontal component k_h of the pseudo-static coefficient until a unit pseudo-static safety factor was achieved. Comparable values of $k_{h,c}$ were detected in the case of horizontal acceleration directed downstream ($k_{h,c} = 0.175$) or upstream ($k_{h,c} = 0.176$) assuming, in both cases, a vertical seismic coefficient directed upwards ($k_v = -0.5k_h$).

The analysis results are shown in Figure 4 where bold solid lines were used to describe the ranges of the mean values of u_x (Fig. 4a,c) and u_y (Fig. 4b,d) computed, using all the selected empirical relationships, for the downstream shell of the dam; lower values were always predicted for the upstream shell. The small arrows at the top of some of the solid lines plotted in Figure 4, when available, denote the upper bound of the predicted permanent displacements. Peak values of the horizontal and vertical permanent displacement were obtained at the *CLS* using accelerogram #2 and are equal to about $u_x = 45$ cm and $u_y = 18$ cm.

4.2. Dynamic time-domain analysis

Some of the results of the dynamic analyses are shown in Figure 5 in terms of contours of vertical and horizontal components of permanent displacement evaluated using the records #5 and #6, which resulted the most severe input motions for the *CLS* and the *LLS*, respectively. For the cases of Figure 5, as for all the other analyses carried out with the other input motions (Tab. 1), permanent displacements are concentrated in the shallowest areas of the dam section and, generally, the larger displacements occur in the upstream shell of the dam, without intersecting the core. The maximum value of permanent displacements was obtained for the *LLS* in the analyses carried out using input motion #6, probably due to its large energy content (Tab. 1). The largest value of the vertical permanent displacement at the crest of the dam is about 16 cm which is much smaller than the service freeboard.

5. Concluding remarks

The seismic behaviour the San Pietro dam was examined through pseudo-static, simplified displacements and dynamic 2D analyses carried out using the computer code FLAC 2D v.7.0. Two sets of input motions were properly selected for the *Life Safety Limit State* and for the *Collapse Limit State*. All the analyses lead to expected permanent displacements smaller than 50 cm with a vertical component, at the crest of the dam, of about 16 cm which is smaller than the service freeboard of the dam.

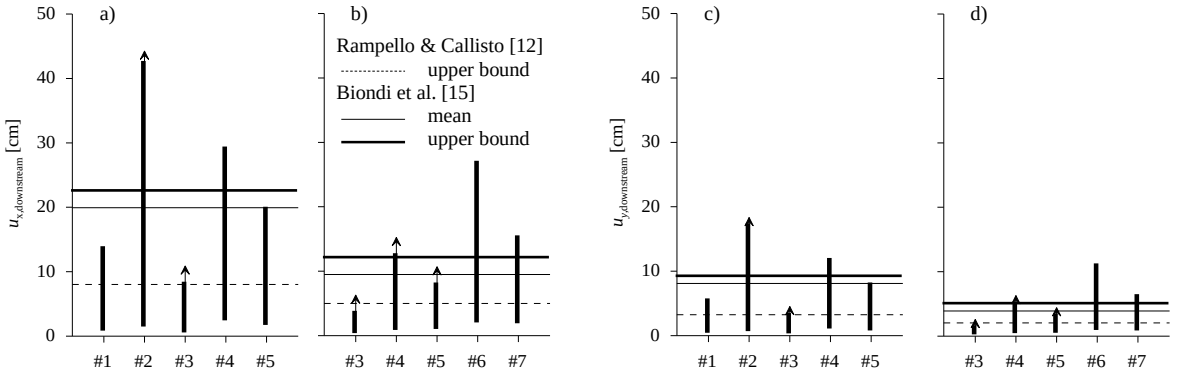

Fig. 4. Horizontal (a,b) and vertical (c,d) component of the expected displacements evaluated for the *CLS* (a,c) and the *LLS* (b,d).

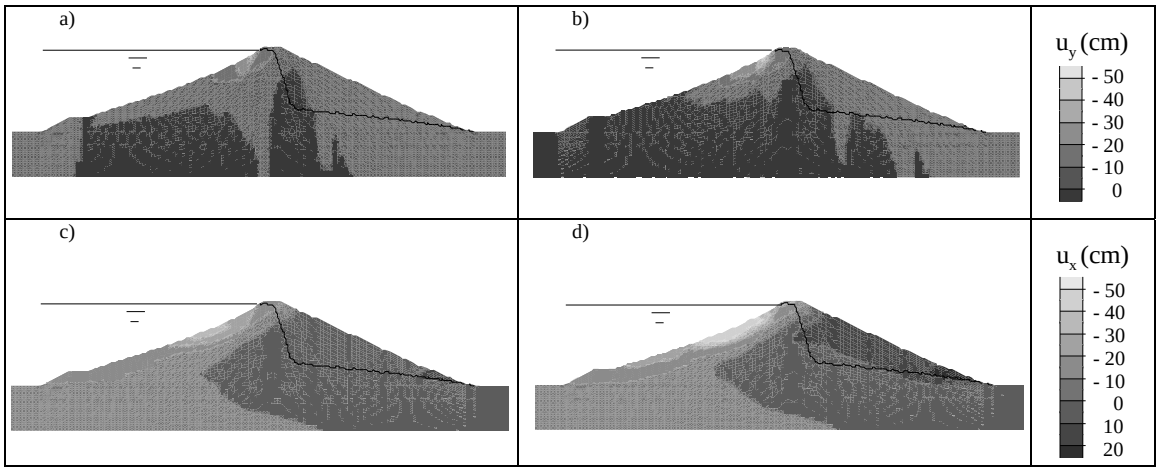

Fig. 5. Contours of vertical (a,b) and horizontal (c,d) components of permanent displacements computed for the *CLS* and the *LLS*.

References

[1] Calabresi G., Rampello S., Callisto L., Cascone E., Diga S. Pietro sul fiume Osento. Verifica delle condizioni di stabilità e analisi del comportamento in condizioni sismiche, Università di Roma "La Sapienza" Contratto di Ricerca con il Consorzio per la Bonifica della Capitanata, 2004.
[2] ITASCA, FLAC – Fast Lagrangian Analysis of Continua – Version 7.0. User's Guide, Itasca Consulting Group, Minneapolis, USA, 2011.
[3] D.M. 14-01-2008. Norme Tecniche per le Costruzioni – GURI 04-02-2008 n°29.
[4] D.M. 26-06-2014. Norme tecniche per la progettazione e la costruzione degli sbarramenti di ritenuta (dighe e traverse) – GURI 08-07-2014 n°156.
[5] ITACA – http://itaca.mi.ingv.it/ItacaNet/itaca10_links.htm.
[6] PEER – http://peer.berkeley.edu/smcat.
[7] Joyner W.B., Boore D.M., Peak horizontal acceleration and velocity from strong motion records including records from the 1979 Imperial Valley, California, earthquake, Bulletin of the Seismological Society of America, 71 (1981) 2011-2038.
[8] Spallarossa D., Barani S., Disaggregazione della pericolosità sismica in termini di M-R-ε, Convenzione INGV-DPC 2004-2006, Progetto S1 "Task 1 – Completamento delle elaborazioni relative a MPS04", Deliverable D14, 2007.
[9] Bommer J.J., Acevedo A.B., The use of real earthquake accelerograms as input to dynamic analysis. J. Earthquake Engineering, 8, Special issue 1 (2004) 43-91.
[10] Pagliaroli A., Lanzo G., Selection of real accelerograms for the seismic response analysis of the historical town of Nicastro (Southern Italy) during the March 1638 Calabria earthquake. Eng. Struct. 30 (2008) 2211-2222.
[11] Crespellani T., Madiai C., Vannucchi G., Earthquake destructiveness potential factor and slope stability, Geotechnique 48(3) (1998) 411-419.
[12] Rampello S., Callisto L., Stabilità dei pendii in condizioni sismiche, In Opere Geotecniche in Condizioni Sismiche. XII Ciclo di Conferenze di Meccanica e Ingegneria delle Rocce, 2008, pp. 241-271.
[13] Saygili, G., Rathje, E.M., Empirical predictive models for earthquake-induced sliding displacements of slopes, Journal of Geotechnical and Geoenvironmental Engineering ASCE 134(6) (2008) 790-803.
[14] Madiai C., Correlazioni tra parametri del moto sismico e spostamenti attesi del blocco di Newmark, Rivista Italiana di Geotecnica (2009) 23-43.
[15] Biondi G., Cascone E., Rampello S., Valutazione del comportamento dei pendii in condizioni sismiche. Rivista Italiana di Geotecnica (2011) 11-34.
[16] Ausilio E., Silvestri F., Tropeano G., Simplified relationships for estimating seismic slope stability. Proc. ISSMGE – ETC12 Workshop on geotechnical aspects of EC8, Madrid, Spain, 2007.
[17] Rathje, E.M., Antonakos, G., A unified model for predicting earthquake-induced sliding displacements of rigid and flexible slopes, Engineering Geology 122 (2011) 51-60.
[18] Bray, J.D., Travasarou, T., Simplified procedure for estimating earthquake-induced deviatoric slope displacements, Journal of Geotechnical and Geoenvironmental Engineering ASCE 133(4) (2007) 381-392.